Computations of nonlinear energy transfer for JONSWAP and empirical wind wave spectra

W. Sell and K. Hasselmann
Institute of Geophysics, University of Hamburg

Hamburg
Institut für Geophysik
[um 1972]

1. Integration method

This report contains an unedited compilation of the original CR-output of the nonlinear energy transfer rates evaluated for a series of gravity-wave spectra on the NCAR CDC 6600 computer. Many of the cases correspond to field spectra measured during the Joint North Sea Wave Project (JONSWAP). The integration method follows Hasselmann [3], with the following improvements:

(a) The integrable singularity along the edges of the integration region, caused by projection of the resonance surface in R4 onto the integration subspace in R3, was removed and treated analytically prior to numerical integration. This reduced the number of grid points needed in the innermost integration loop (NAL1 below)

(b) The symmetry properties of the transfer integral [2]

$$\frac{\partial n_4}{\partial t} = \int \sigma \left[n_1 n_2 n_3 + n_1 n_2 n_4 - n_1 n_3 n_4 - n_2 n_3 n_4 \right] d\underset{\sim}{k}_1 \, d\underset{\sim}{k}_2 \, d\underset{\sim}{k}_3 \, ,$$

$$n(\underset{\sim}{k}) = [\text{energy spectrum } E(\underset{\sim}{k})] / \omega ,$$

were made use of to obtain three independent estimates of $\partial n/\partial t$ for each integration performed. Of these, the first corresponds to $\partial n_4/\partial t$ as computed previously, whereas the other two are derived from the changes occurring in n_1 and n_3 for each "collision process" causing an incremental change in n_4 . (The n_2 -term did not yield a further estimate independent of $\partial n/\partial t$ on account of the assumed axial symmetry of the spreading functions, which had already been exploited in integrating with respect to $\underset{\sim}{k}_1$ and $\underset{\sim}{k}_2$). The mean value

$$\frac{\partial n}{\partial t} = \frac{1}{4}\left[2\frac{\partial n_1}{\partial t} + \frac{\partial n_3}{\partial t} + \frac{\partial n_4}{\partial t}\right]$$

of all three terms proved to be considerably more stable numerically than the individual estimates and also conserved total energy and momentum to a much higher accuracy. These advantages were particularly marked at high wavenumbers, where the previous computations by Hasselmann [3] and — to a lesser degree — Cartwright (unpublished) became inaccurate (cf. first four figures).

2. Figures

1. The first four figures show an intercomparison of the case D3B and corresponding computations by Cartwright. The latter were obtained by single $\partial n_4/\partial t$ -integrations, but by a numerical method differing from [3].

2. The remaining figures correspond to the cases listed in the following, each case consisting of figures in the following sequence:

   a. data sheet (missing in earlier runs)

   b. spectrum E(f)

   c. normalised spreading function

   d. a series of two dimensional source functions $\partial E(f,\theta)/\partial t$ for given θ , where ...... = $\frac{\partial E_1}{\partial t}$, $\frac{\partial E_2}{\partial t}$

—— —— = $\frac{\partial E_3}{\partial t}$

---- = $\frac{\partial E_4}{\partial t}$

———— = $\frac{\partial E}{\partial t} = \frac{1}{4}\left(2\frac{\partial E_1}{\partial t} + \frac{\partial E_3}{\partial t} + \frac{\partial E_4}{\partial t}\right)$

e. the one dimensional source function

$$\frac{\partial \hat{E}}{\partial t}(f) = \int \frac{\partial E}{\partial t}(f, \theta)\, d\theta$$

f. the one dimensional momentum source function

$$\frac{\partial \hat{M}}{\partial t} = \int \frac{\partial E}{\partial t}(f, \theta)\, \frac{\omega}{g} \cos\theta \, df$$

(missing in earlier runs)

g. the set of mean two dimensional source functions

$\frac{\partial E}{\partial t}(f, \theta)$ for fixed θ (in earlier runs $\frac{\partial E_4}{\partial t}$,
denoted in the figure caption by "AT K4")

3. Computed Cases

CASE	NAL1	NX	DELXO	XMAX	LFR	NTH	Comments	α	f_m	σ_a	σ_b	γ
							Resolution and numerical stability tests (Piers-Mosk.spect					
D2B*	18	23	.23	10.6	17	9	low-resolution version of D3B. Scattered, but means agree with D3B					
D3B	18	34	.14	6.0	20	7	good compromise between resolution and run time					
D4B*	36	23	.23	10.6	17	9	higher angular resolution than D3B. Little change					
D5B*	9	15	.34	8.0	17	9	very low angular resolution. Scattered, means also deviate from D3B					
							3 typical JONSWAP spectra					
JN5*	18	34	.14	6.0	20	7	mean JONSWAP spectrum	.01	.3	.07	.09	3.3
J6B	18	34	.14	6.0	24	7	more sharply peaked spectrum	.01	.3	.05	.07	4.2
J8B	18	34	.14	6.0	24	7	less sharply peaked spectrum	.01	.3	.12	.12	2.7
							6 individual JONSWAP spectra					
R1C*	18	34	.14	6.0	20	7		.0156	.371	.104	.104	3.67
R2C*	18	34	.14	6.0	20	7		.0205	.416	.060	.100	3.24
R3C*	18	34	.14	6.0	20	7		.0100	.354	.068	.123	6.99
R4C*	18	34	.14	6.0	20	7		.0204	.349	.057	.077	3.86
R5C*	18	34	.14	6.0	20	7		.0155	.421	.072	.092	3.42
R9C*	18	34	.14	6.0	20	7		.0091	.263	.085	.083	3.06
							3 Pierson-Moskowitz cases					
PMB*	18	23	.14	2.4	20	7	same as PNB with badly chosen frequency mesh Points scatter. Relevant only for compariso with PMC.					
PMC*	18	34	.14	6.0	20	7	same as PMB but with extension of x-integrat plane from 2.4 to 6. Little change.					
PNB*	18	23	.14	2.4	20	7	better computation than PMB or PMC					
							Square spectrum with ω^{-5} tail					
DEM	12	23	.23	10.6	17	5	shows evolution of peak within the flat part of the spectrum					

General Comments:

*1. In earlier runs, a factor of 2 is missing in the ordinate scales for the one dimensional transfer rates. These runs are marked by * .

2. Units are in m and sec, with the exception of cases D2B-D5B, which are in ft. and sec, the spectrum being normalised such that $\int \hat{E}(f)\,df = 1\ ft^2$ (scaling rules are given in [3]). Spectra represent mean square wave height densities with respect to frequency in Hz and propagation direction in radians.

3. All spreading functions $S(\theta)$ are half-plane $\cos^2\theta$ distributions with the exception of cases D2B-D5B, for which

$$S(\theta) = \frac{8}{5\pi} \cos^6 \frac{\theta}{2} \quad (-\pi \leq \theta \leq \pi)$$

4. Notation:

The integration was performed with respect to the variables

α_1 = angle of vector $\underset{\sim}{k}_1$ relative to $\underset{\sim}{k}_4$,

x_1 = $|\underset{\sim}{k}_1|/|\underset{\sim}{k}_4|$

and x_2 = $|\underset{\sim}{k}_2|/|\underset{\sim}{k}_4|$ (cf.[2]).

Then NAL1 = no. of α_1 grid points (between 0 and π)

NX = no. of x_1 and x_2 grid points

DELX0 = initial mesh size of x_1 and x_2 integration (increases nonlinearly with x_1 and x_2)

XMAX = max. value of x_1 and x_2

LFR = no. of output frequency points (listed explicitly as "stutzpoints" on data sheet)

NTH = no. of output angles θ (θ increases in increments of 15° in all cases except DEM, where the increment is 20°)

The JONSWAP spectra are defined in terms of the five parameters

α, f_m, σ_a, σ_b and γ:

$$\hat{E}(f) = \frac{\alpha g^2 f^{-5}}{(2\pi)^4} \exp(-1.25\,\nu^{-4})\, \gamma^{\exp\left(-\frac{1}{2}\left(\frac{\nu-1}{\sigma}\right)^2\right)}$$

where $\nu = f/f_m$, $\sigma = \begin{cases} \sigma_a & \text{for } \nu \le 1 \\ \sigma_b & \text{for } \nu \ge 1 \end{cases}$

Acknowledgments

All calculations were carried out on the CDC 6600 and CDC 6700 computers of the National Center for Atmospheric Research, Boulder, Colorado, which is sponsored by the U.S. National Science Foundation. The authors are grateful for use of these facilities and the generous assistance provided by the NCAR staff.

References

Hasselmann, K. On the non-linear energy transfer in a gravity-wave spectrum:

1. (1962) Part 1: General Theory. J. Fluid Mech. 12, 481-500

2. (1963) Part 2: Conservation theorems, wave-particle correspondence, irreversibility. J. Fluid Mech. 15, 273-281

3. (1963) Part 3: Computation of the energy flux and swell-sea interaction for a Neumann spectrum. J. Fluid Mech. 15, 385-398

4. Barnett, T.P., E. Bouws, H. Carlson, D. Cartwright, J.A. Ewing, H. Geinapp, D.E. Hasselmann, K. Hasselmann, P. Krusemann, A. Meerburg, K. Richter, W. Sell and H. Walden (1971) Measurements of wind-wave growth and swell decay in the North Sea (Joint North Sea Wave Project - JONSWAP), AGU, Washington, April 1971, and IUGG, Moscow, Aug. 1971 (to be published in Deutsche Hydrogr. Zeitschrift)

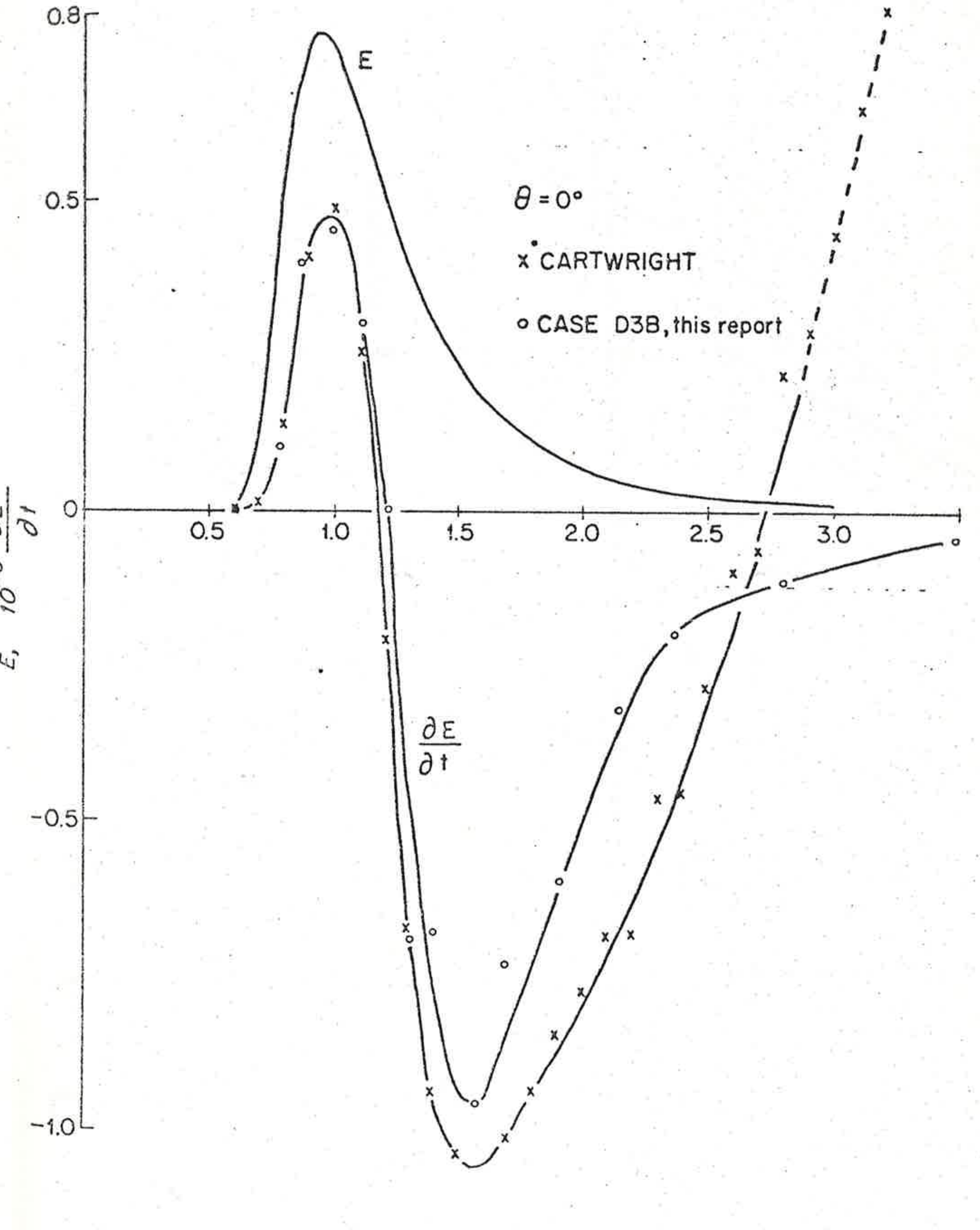

0.8
0.5
0
-0.5
-1.0
0.5
1.0
1.5
2.0
2.5
3.0
E
$\theta = 0°$
x CARTWRIGHT
o CASE D3B, this report
$\frac{\partial E}{\partial t}$
$E,\ 10^{-3}\ \frac{\partial E}{\partial t}$

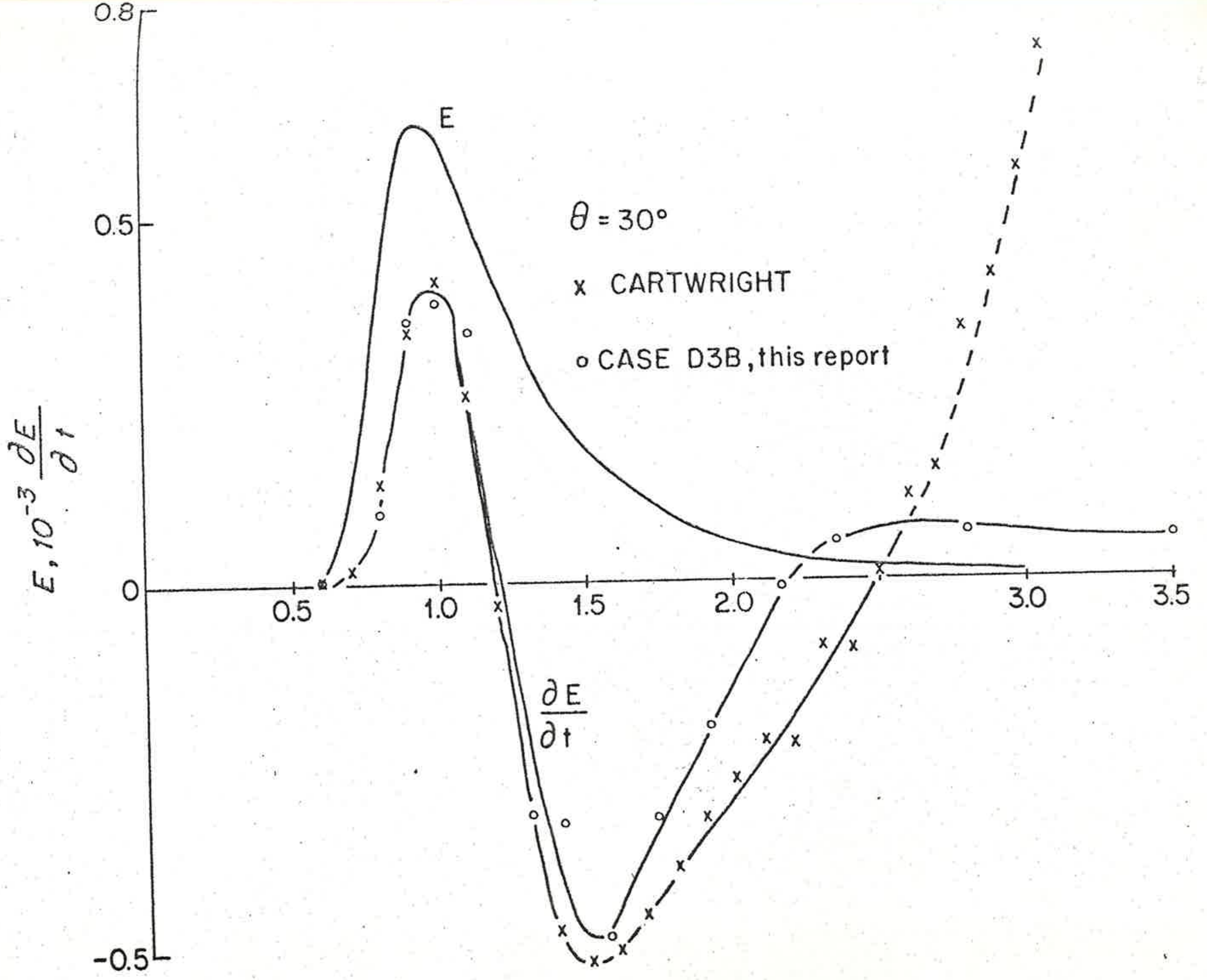

E
θ = 30°
x CARTWRIGHT
o CASE D3B, this report
∂E/∂t
E, 10⁻³ ∂E/∂t
0.8
0.5
0
-0.5
0.5
1.0
1.5
2.0
3.0
3.5

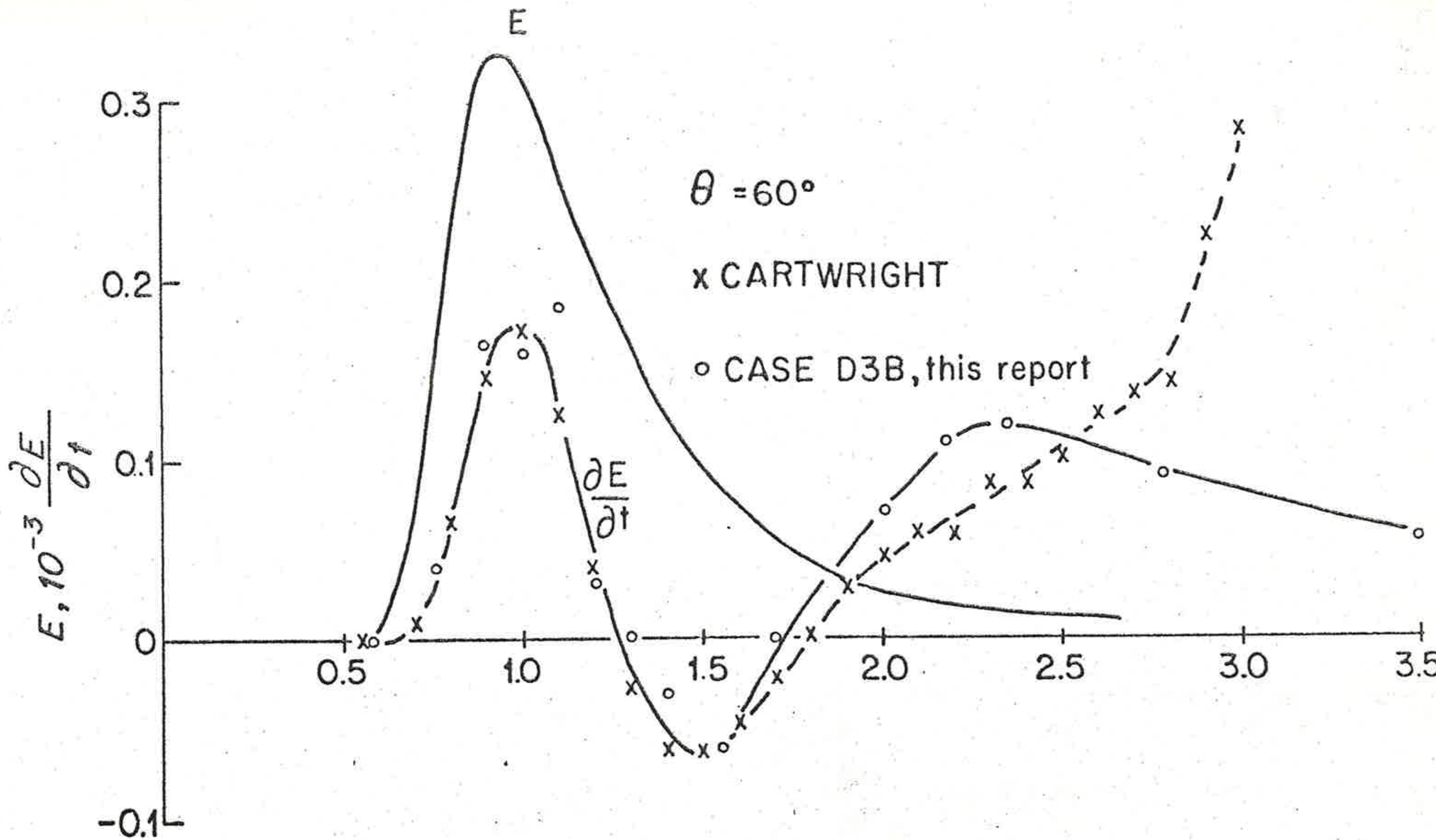

E
0.3
0.2
0.1
0
-0.1
$E, 10^{-3} \frac{\partial E}{\partial t}$
$\frac{\partial E}{\partial t}$
θ =60°
x CARTWRIGHT
o CASE D3B, this report
0.5
1.0
1.5
2.0
2.5
3.0
3.5

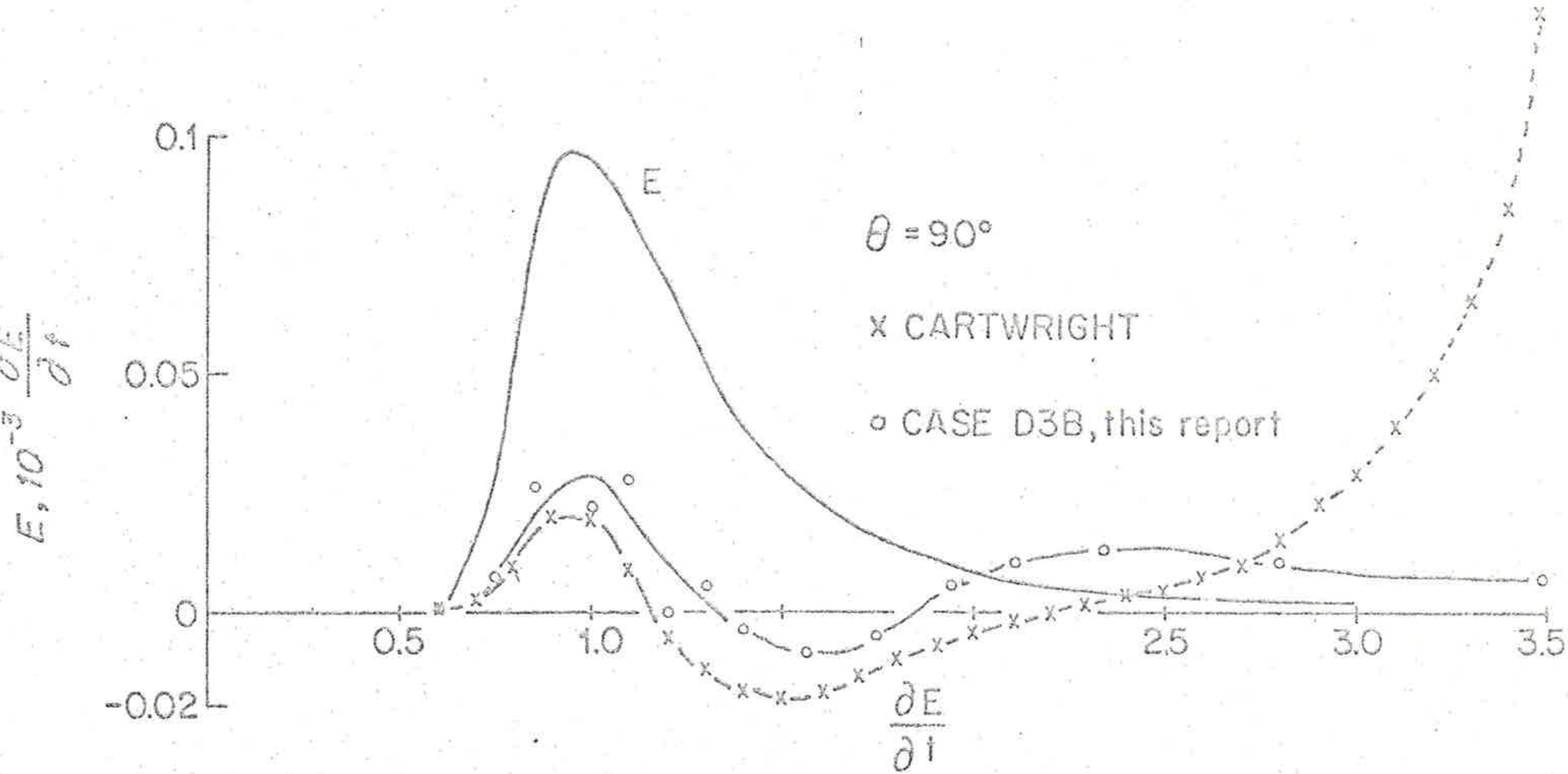

+ ca. 250 S. Diagramme